



MINISTÉRIO DA CIÊNCIA E TECNOLOGIA

INSTITUTO NACIONAL DE PESQUISAS ESPACIAIS

INPE-11296-PRE/6733

**STABILIZATION OF A SPACE VEHICLE USING THE SIGN OF
ANGULAR VELOCITY SENSORS AND GAS JETS AS THRUSTERS**

Wilson Custódio Canesin Da Silva*
Paulo Giácomo Milani**

ADVANCES IN SPACE DYNAMICS 4: CELESTIAL MECHANICS AND ASTRONAUTICS,
H. K. Kuga, Editor, 171-178 (2004).
Instituto Nacional de Pesquisas Espaciais – INPE, São José dos Campos, SP, Brazil.
ISBN 85-17-00012-9

INPE
São José dos Campos
2004

**ESTABILIZATION OF A SPACE VEHICLE USING THE SIGN OF
ANGULAR VELOCITY SENSORS AND GAS JETS AS THRUSTERS**

Wilson Custódio Canesin Da Silva *
Paulo Giácomo Milani**

***Braz Cubas University - UBC** , Mogi das Cruzes -S.Paulo, Residential Address:
Rua Guilherme de Almeida , 91 – CEP-12.245-100, Jd.Renata, São José dos
Campos – S. Paulo – Brazil
E-mail: canesin@iconet.com.br -phone: +55(12)3922-5037,

****National Institute of Space Research – INPE**, P.O.Box 515,
12.227-010 Avenida dos Astronautas, 1758, São José dos Campos – SP, Brazil
E-mail: milani@dem.inpe.br , phone: +55(12)3945-6181

ABSTRACT

This work presents a modification implemented in the stabilization system of a microgravity platform, the SubOrbital Platform – PSO₁. The hardware architecture of the original system has not been modified and was composed of a Girometric Block, an On Board Computer and a Gas Jet System (hidrazine). On the other hand the software has been altered to consider only the signal of the angular velocities instead of the intensity of these same velocities. The algorithm used is presented and simulations of the system are executed. At the end the results of the simulations are presented.

1.-Introduction

The SubOrbital Platform Project has as one of its objectives to test some hardware equipments developed by INPE and the national industry of Brazil and additionally provide the environment for the execution of experiments in microgravity conditions. The Project consists in launching a sounding rocket of the Sonda III type carrying a platform of 2.7m high and 300mm diameter. The platform follows a parabolic trajectory of 300km of apogee from a launch base in the city of Natal, RN, in northeast Brazil, the Launch Center of Barreira do Inferno. The PSO is equipped with gyroscopes and accelerometers among other sensors. The first ones

measure the spin rates of the platform and the last ones measure its accelerations. The alignment of the sensors was made such that it enables the measurement in relation to the 3 principal axes of the platform. Due to a matter of measurement scales the gyroscopes can only read angular rates below 3.4 rpm (or $20^{\circ}/s$) but at the beginning of the stabilization phase the angular rates are in the order of 180 rpm and so much higher than the end of scale limit. Once it is not possible to read the intensity of the rates a control technique is presented that uses only the signs of the angular rates, not bothering with its intensity value and by means of a control strategy the thrusters (gas jets) are fired until the complete stabilization of the platform is obtained. Another study similar to this one has already been presented by Silva and Souza, 2002.

2. – The Layout of the Platform

The SubOrbital Platform has its inferior part in the form of a cylinder and its superior part is a cone as in Fig. 1. Its 4 thrusters A, B, C and D are arranged in a plane ($X'Y'$) placed at a distance “a” from the center of mass (XY) of the platform. All of the thrusters are aligned in the directions indicated by the arrows.

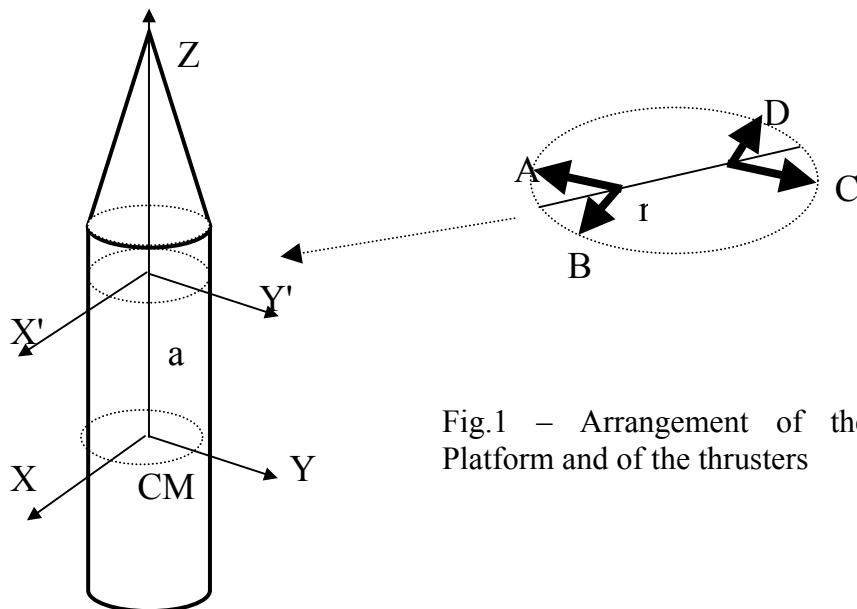


Fig.1 – Arrangement of the PSO Platform and of the thrusters

3.- Gyroscope subsystem

The angular rates in the 3 axis of the PSO are measured by a system composed of 2 gyroscopes. Each one is able to make measurements in 2 axis. They are mounted on

a block that provides dumping and alignment following angles of 45° with the spin axis (Z) of the platform. The values W_{x1} , W_{y1} , W_{x2} , W_{y2} are the measurements of the components of the angular velocities in the reference systems of the two sensors (gyros) and S1 and S2 are their spin axis directions.

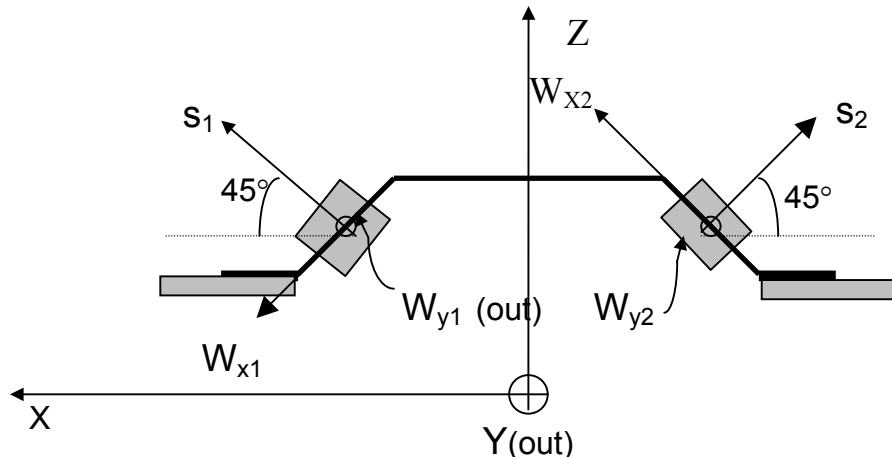


Fig.2- Gyro block arrangement

The transformation from the system of the gyros (Fig. 2) to the system of the platform (Fig. 1) is given by the following relations:

$$W_{XPSO} = (W_{x2} + W_{x1})\cos\beta / \sqrt{2} + (W_{y1} + W_{y2})\sin\beta / 2$$

$$(2.1) \quad W_{YPSO} = -(W_{x2} + W_{x1})\sin\beta / \sqrt{2} + (W_{y1} + W_{y2})\cos\beta / 2$$

$$W_{ZPSO} = (W_{x2} - W_{x1}) / \sqrt{2}$$

where one includes an angle $\beta=25^\circ$ due to the relative position of the block inside the platform structure. This angle corresponds to a rotation of the Gyro Block around its Z axis, causing a misalignment β of the axis x and y of the block in relation to the X and Y axis of the PSO₁.

4.- Equations of the Forces and Torques

Cutting transversal along the PSO and passing by the plane (X',Y') that contains the thrusters it is possible to observe the configuration of Fig. 3 and the form how each one of the thrusters: F_A , F_B , F_C , F_D actuate on the system (Table 1).

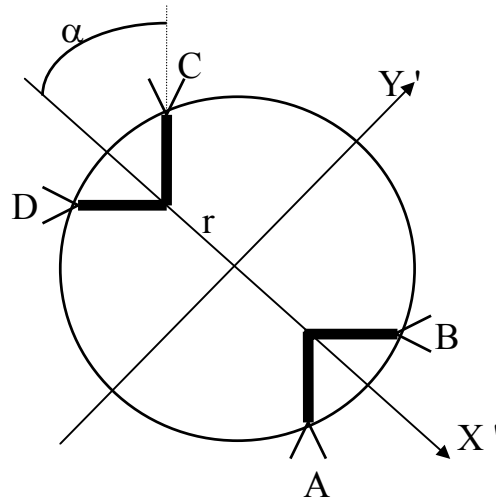


Fig.3: Corte transversal do sistema propulsivo

These forces when decomposed along the axis X and Y of the PSO result in the expressions as follows:

Table 1: components of the propulsive forces

Forças	X	Y	z
F_A	$-F \cos \alpha$	$F \sin \alpha$	0
F_B	$-F \cos \alpha$	$-F \sin \alpha$	0
F_C	$F \cos \alpha$	$-F \sin \alpha$	0
F_D	$F \cos \alpha$	$F \sin \alpha$	0

The torques due to the 4 thrusters are:

$$\mathbf{T}_i = \mathbf{d} \times \mathbf{F}_i \tag{3.1}$$

The distances d and d' (see Fig.1) are given by:

$$\mathbf{d} = r\mathbf{i} + a\mathbf{k} \quad \mathbf{d}' = -r\mathbf{i} + a\mathbf{k} \tag{3.2}$$

Calculating the vector product it is possible to arrive at Table 2:

Table 2: Torques due to the 4 thrusters

Torques	X	Y	Z
T_A	$-F a s\alpha$	$-F a c\alpha$	$F r s\alpha$
T_B	$F a s\alpha$	$-F a c\alpha$	$-F r s\alpha$
T_C	$F a s\alpha$	$F a c\alpha$	$F r s\alpha$
T_D	$-F a s\alpha$	$F a c\alpha$	$-F r s\alpha$

Making a combination of the torques of the thrusters 2 at a time it is possible to obtain torques in the 3 axis of the platform.

Table 3: torques in the 3 axis of the PSO platform

Signs of the torques	Thrusters used	TX	TY	TZ
- TX	A , D	$-2.a.F.s\alpha$	0	0
+ TX	C , B	$2.a.F.s\alpha$	0	0
- TY	A , B	0	$-2.a.F.c\alpha$	0
+TY	C , D	0	$2.a.F.c\alpha$	0
+TZ	A , C	0	0	$2.r.F.s\alpha$
- TZ	B , D	0	0	$-2.r.F.s\alpha$

Table 4 presents also the signs of the angular velocities in all the possible directions for the case of using the thrusters in pairs, the torques being oposed to the angular velocities and the thrusters that are used in each one of these cases.

Tabela 4 – Syntesis of the actuation system

Angular velocities	Torques	Thrusters to use
$w_x > 0$	$-T_X$	A , D
$w_x < 0$	$+T_X$	C , B
$w_y > 0$	$-T_Y$	A , B
$w_y < 0$	$+T_Y$	C , D
$w_z > 0$	$-T_Z$	B , D
$w_z < 0$	$+T_Z$	A , C

5.- Strategy of stabilization of the platform

As mentioned before the strategy for the decision of the thrusters to fire is based simply in the use of the signs of the angular velocities measured by the gyroscopes according to the equations in 3.1.

Table 5 – Control logic with the signs of the gyros

Conversion from the system of the gyros to the one of the PSO		
$WX = (WX2+WX1) \cos\beta/\sqrt{2} + (WY1 + WY2)\text{sen}\beta / 2$		
$WY = - (WX2+WX1) \text{sen}\beta/\sqrt{2} + (WY1 + WY2)\cos\beta / 2$		
$WZ = (WX2 - WX1) / \sqrt{2}$		
a)	Se $WX1, WX2, e WY1,2 > 0,$	then $WX > 0$
b)	Se $WX1, WX2, e WY1,2 < 0,$	then $WX < 0$
c)	Se $WX1, WX2 > 0, e WY1,2 < 0,$	then $WY < 0$
d)	Se $WX1, WX2 < 0, e WY1,2 > 0,$	then $WY > 0$
e)	Se $WX2 > 0 e WX1 < 0,$	then $WZ > 0$
f)	Se $WX1 > 0 e WX2 < 0,$	then $WZ < 0$

In the beginning of the stabilization maneuver $WX2 > 0$ and $WX1 < 0$ what corresponds to $Wz > 0$ as in the case “e” above. This is the nominal case in the mission. Afterwards depending on the evolution of the dynamics of the platform the other cases can happen. This way the stabilization around the Z axis is accomplished first and is followed by stabilization around the X and Y axis. This strategy of control considers the stabilization of the platform even if the initial angular rates are reversed ($WZ < 0$).

6.- Tests executed

For the execution of this test it has been considered the “worst case scenario”, trying to evaluate the robustness of the method and the possibility of its use in the real system to be flown onboard PSO₁. This way high initial rates have been used, much above the saturation level of the gyros. The values used were:

- $WX = 18^\circ/s, WY = 18^\circ/s e WZ = 1440^\circ/s$

The dead zone around zero when the control stops action around na axis was used:

- Epsilon = $1^\circ/s$ (stop value of the stabilization)

What resulted in:

- Stabilization time around: 300s.
- Residual accelerations of the order: $10^{-5}g$

In analysing the results presented in the Annex 1 it is possible to note the control strategy adopted, reducing first the angular rates around the longitudinal or Z axis and then around the other two, the transversal axis.

7.-Conclusions and final comments

The new logic of stabilization that has been tested for initial angular rates and with gyros saturated worked efficiently, enabling the stabilization of the platform using only the 3 signs of the angular rates of the platform. The stabilization time of the platform resulted large (300s) because the initial rates were also large. In the real life case where the rates are smaller, of the order of $0.2^{\circ}/s$ the stabilization occurred in around 2 minutes.

8 – Bibliography

Silva, W.C.C., de Souza, L.C.G. ; Spin Reduction of Space Vehicles Using Gas Jets.- Dynamics and Control of Systems and Structures in Space 2002. Pages 51-56, July 2002, Cranfield University Press. (ISBN 1 871 315 79 4).

Annex 1: Simulation results

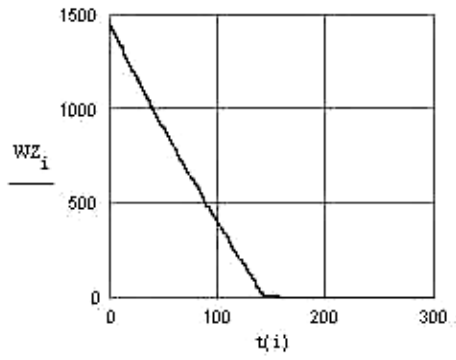


Fig. 1 - Wz in o/s

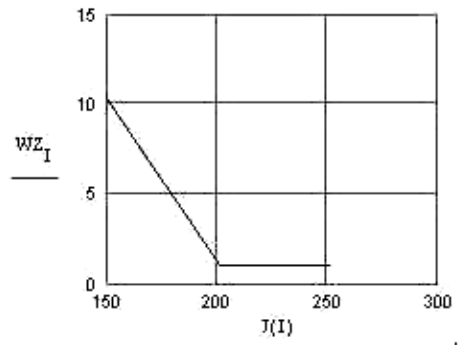


Fig. 2 - Wz in o/s

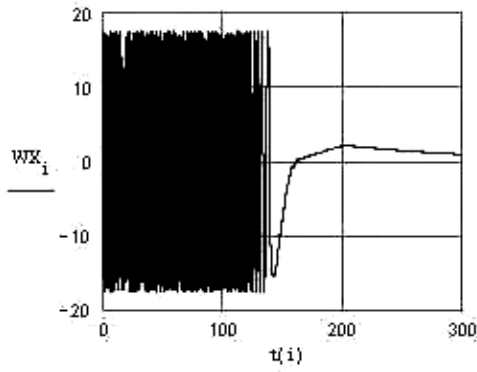


Fig. 3 - Wx in o/s

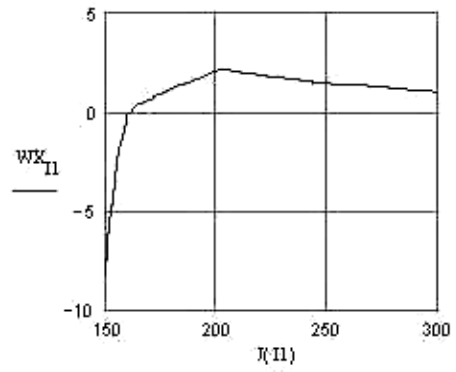


Fig. 4 - Wx in o/s

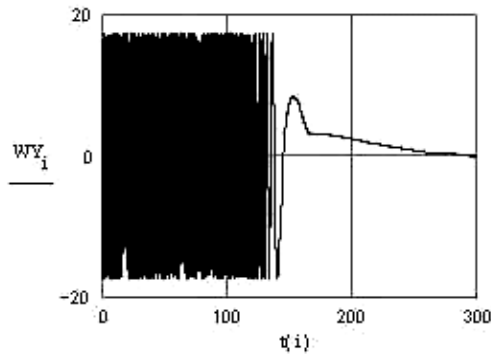


Fig. 5 - Wy in o/s

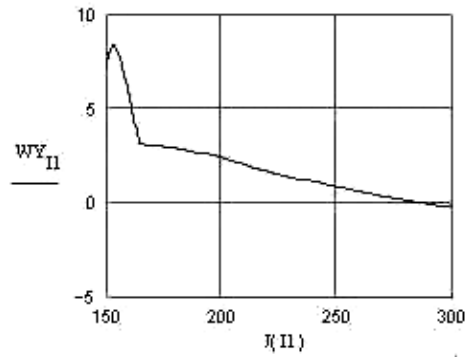


Fig. 6 - Wy in o/s

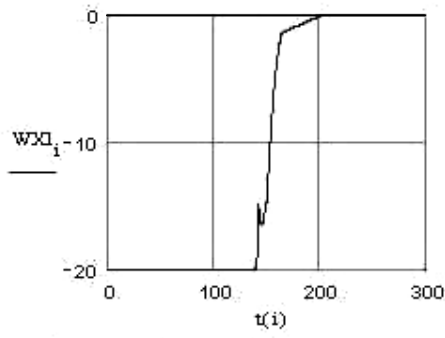


Fig. 7 - Wx1 in o/s from Gyro 1

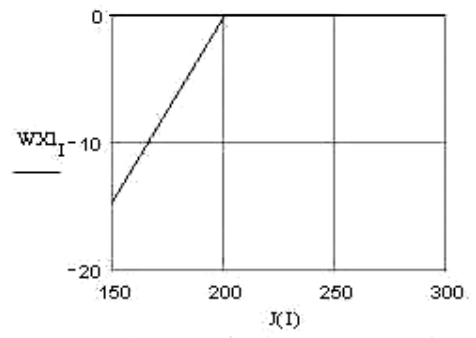


Fig. 8 - Wx1 in o/s from Gyro 1

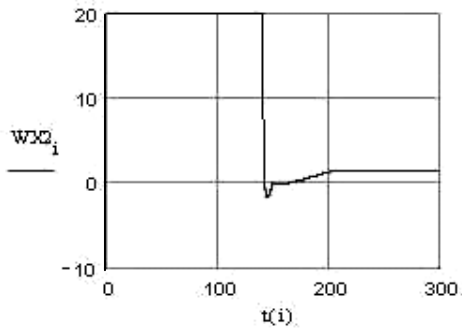


Fig. 7 - Wx2 in o/s from Gyro 2

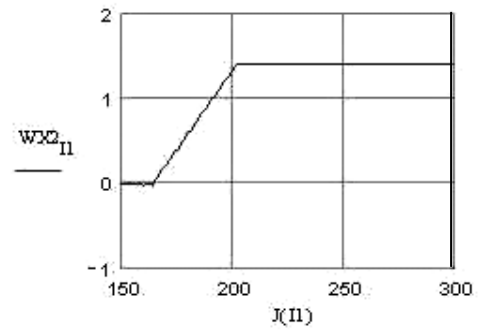


Fig. 8 - Wx2 in o/s from Gyro 2

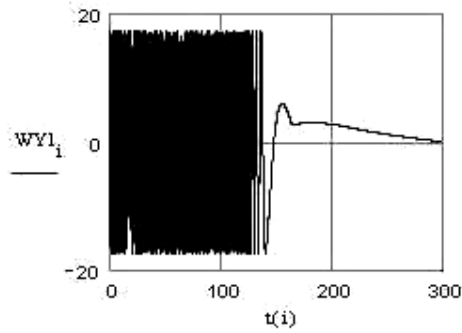


Fig. 7 - Wy1-2 in o/s from Gyro 1

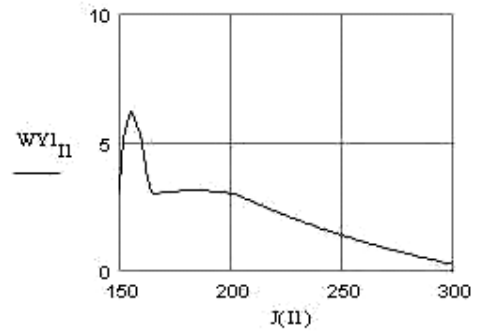


Fig. 8 - Wy1-2 in o/s from Gyro 1